Diabetogenic T cells recognize insulin bound to IA^{g7} in an unexpected, weakly binding register

Brian D. Stadinski[a,b,1], Li Zhang[c], Frances Crawford[a,b], Philippa Marrack[a,b], George S. Eisenbarth[a,c], and John W. Kappler[a,b,2]

[a]Integrated Department of Immunology, University of Colorado and National Jewish Health, Denver, CO 80206; [b]Howard Hughes Medical Institute, National Jewish Health, Denver, CO 80206; and [c]Barbara Davis Center for Childhood Diabetes, Aurora, CO 80045

Contributed by John W. Kappler, May 10, 2010 (sent for review April 28, 2010)

A peptide derived from the insulin B chain contains a major epitope for diabetogenic $CD4^+$ T cells in the NOD mouse model of type 1 diabetes (T1D). This peptide can fill the binding groove of the NOD MHCII molecule, IA^{g7}, in a number of ways or "registers." We show here that a diverse set of NOD anti-insulin T cells all recognize this peptide bound in the same register. Surprisingly, this register results in the poorest binding of peptide to IA^{g7}. The poor binding is due to an incompatibility between the p9 amino acid of the peptide and the unique IA^{g7} p9 pocket polymorphisms that are strongly associated with susceptibility to T1D. Our findings suggest that the association of autoimmunity with particular MHCII alleles may be do to poorer, rather than more favorable, binding of the critical self-epitopes, allowing T-cell escape from thymic deletion.

diabetes | autoimmunity | tolerance | self-antigens | antigen presentation

The development of type 1 diabetes (T1D) in NOD mice and humans is associated with certain alleles of MHCII (1–3). These alleles present sets of peptides distinct from those presented by other MHCII alleles (4, 5), thus their association with T1D may be because they are better than other MHCII alleles at presentation of peptides derived from pancreatic islet β-cell proteins (6). However, tests of this and other hypotheses about the role of MHCII in T1D require a precise identification of the peptides recognized by pathogenic $CD4^+$ T cells.

Peptides bind in an extended conformation to a groove of MHCII. The binding involves a nonamer of the peptide (p), in which the side chains of "anchor" amino acids at positions p1, p4, p6, and p9 interact with corresponding pockets in the groove (7). Polymorphic MHCII residues lining the binding groove influence the preference of each pocket for particular peptide side chains, providing each MHCII allele with a unique preferred peptide-binding motif that dictates the position or "register" of the peptide in the groove. However, the specificities of these pockets are not absolute, and so a peptide may bind in more than one register, with the hierarchy of registers determined by how well the pockets accept the anchor residues. The register of the peptide affects which of its side chains are pointing out of the MHCII groove and hence interaction with T cell receptors. Thus individual peptide-responsive T cells will recognize the peptide bound to MHCII in only one of the possible registers.

The NOD mouse has a single MHCII molecule, IA^{g7}, which is essential for the development of disease (8). Polymorphisms in the IA^{g7} β-chain (9) shape the p9 binding pocket (10, 11) and contribute to a side chain preference distinct from that of other IA alleles (6). In particular, an Asp-to-Ser alteration at IA^{g7} β57 disrupts a conserved salt bridge to an Arg at α76. This allows the positively charged Arg to interact with the peptide amino acid side chain in the p9 pocket (11) and confers a unique preference for binding peptide registers with acidic residues at this position (6).

The insulin B-chain peptide (B:12–23) is recognized by diabetogenic $CD4^+$ T cells in the NOD mouse (12–14) and might bind IA^{g7} in any of four registers. Previous studies have suggested that individual diabetogenic T cells might recognize the peptide in either of two of these registers (15). Of the two remaining registers, one, called register 3 in this study, is predicted to be the least favored of the four possibilities, because it would place an overtly conflicting positively charged arginine side chain in the positively charged p9 pocket.

Here we used an approach we term "register trapping," in which p1 and p9 were optimized for binding to IA^{g7}, to determine which binding registers of the insulin peptide are recognized by a collection of insulin-specific NOD $CD4^+$ T cells. Surprisingly, these T cells all recognized the insulin peptide bound in register 3. IA^{g7}-binding studies with core nonamer peptides confirmed that register 1 and 2 peptides bound to IA^{g7} without anchor optimization, but that the register-3 peptide bound very poorly unless the anchors were changed.

Thus, our findings show that the dominant, diabetogenic $CD4^+$ T-cell response in NOD mice targets insulin bound to IA^{g7} in an unfavorable register. This finding suggests that pathogenic autoreactive $CD4^+$ T cells often target self-antigen epitopes resulting from peptides bound to MHCII in registers with unfavorable binding motifs (16). The combination of poor binding and competition by peptides bound in other registers may prevent sufficient presentation of the critical epitope for thymic deletion, allowing autoreactive T cells targeting these self-antigens to escape negative selection. In the periphery, however, high local expression or modification (17) of the antigen might overcome poor presentation by MHCII, permitting pathogenic T cells to respond to their self-antigen targets and initiate autoimmunity.

Results

Diabetogenic $CD4^+$ T Cell Recognizes Insulin B:12–23 Bound in an Unfavored Register. The insulin B:12–23 peptide may bind to IA^{g7} in any of four registers (Fig. 1*A*). Previous data has suggested that registers 1 and 2 may be most often used by diabetogenic T cells, but that register 3 is disfavored, because of a charge clash between the register 3 arginine at p9 and the positively charged p9 binding pocket of IA^{g7} (15). To be able to study the registers separately, we optimized the peptide amino acids for binding to IA^{g7}, choosing an Arg and Glu at the predicted p1 and p9 positions, respectively, for each of the four registers (Fig. 1*B* and Fig. S1)—a process we call register trapping. These choices were based on the solved structures of IA^{g7} bound to peptides from either hen egg lysozyme (HEL) (10) or glutamic acid decarboxylase (GAD; Fig. S2 *A* and *B*) (11). Besides the nine peptide amino acids that occupy the core of the MHCII groove, amino acids at p−1 are also sometimes impor-

Author contributions: B.D.S. and J.W.K. designed research; B.D.S., F.C., and J.W.K. performed research; B.D.S. and L.Z. contributed new reagents/analytic tools; B.D.S., F.C., P.M., G.S.E., and J.W.K. analyzed data; and B.D.S., P.M., G.S.E., and J.W.K. wrote the paper.

The authors declare no conflict of interest.

Freely available online through the PNAS open access option.

[1]Present address: Department of Pathology, Harvard Medical School, Boston, MA 02115.

[2]To whom correspondence should be addressed. E-mail: kapplerj@njhealth.org.

This article contains supporting information online at www.pnas.org/lookup/suppl/doi:10.1073/pnas.1006545107/-/DCSupplemental.

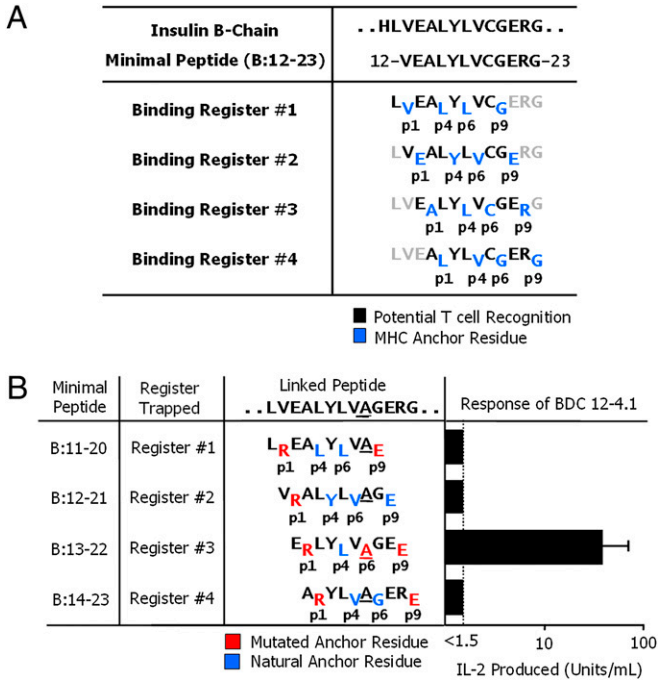

Fig. 1. The BDC 12-4.1 T cell responds to register 3 of the insulin B:12–23 peptide. (*A*) Four possible IA^{g7}-binding registers for the mouse insulin B-chain peptide, B:12–23. Anchor residues are shown in blue, and black residues show the amino acids that potentially contact the T-cell antigen receptor. (*B*) Minimal 10-mer linked peptide versions of the insulin B:12–23(19A) epitope. Each minimal peptide was trapped in a single binding register by a p1Arg and a p9Glu. The substitution of Ala for Cys at B:19 of the peptide is underlined. Red amino acids are the substituted anchor residues. Blue amino acids are the naturally occurring anchor residues. Black amino acids are the possible T-cell epitope residues. Also shown is the stimulation of the BDC 12-4.1 T-cell hybridoma with each of the individual IA^{g7}-linked peptide complexes expressed on the surface of ICAM/$B7^+$ insect cells, assessed by the production of IL-2. Results are the average ± SEM of triplicate wells from five independent experiments.

tant, so peptide constructs also included the relevant amino acid at p−1. Additionally, to avoid potential problems with an unpaired Cys, the B:19 Cys of the peptide was altered to Ala. This mutation does not diminish, and may even enhance, recognition by some T cells (18) (Fig. S3).

We constructed a set of four overlapping 10-mer versions of the insulin B:12–23 minimal peptide, each optimized at p1 and p9 for binding to IA^{g7}, whose C termini were covalently attached via a flexible linker to the N terminus of an insect cell anchored version of IA^{g7} β-chain (19) (Fig. 1*B* and Fig. S1). Each construct was cloned into baculovirus, and the viruses were used to infect SF9 insect cells. All of the recombinant IA^{g7} complexes expressed well on the surface of the infected insect cells (Fig. S4*A*). We assessed the response of a T-cell hybridoma expressing the TCR of the diabetogenic, IA^{g7}/insulin-specific T cell, BDC 12-4.1, to ICAM/$B7^+$ insect cells (20) bearing the IA^{g7}-linked peptide complexes (Fig. 1*B*). Unexpectedly, only the complex that trapped the peptide in register 3 stimulated. This result was surprising because, as stated previously, for the natural insulin peptide in this register, the p9 pocket would have to be occupied by a conflicting Arg (6) (Fig. 1*A*).

Three Other $CD4^+$ T cells Recognize the Insulin Peptide in Register 3. To find out if BDC 12-4.1 was exceptional in its recognition of IA^{g7}/insulin, we analyzed T-cell hybridomas bearing the TCRs from three other islet-infiltrating insulin-responsive $CD4^+$ T cells, AS91, AS150, and I.29 (15). The TCRs on these three T cells differed in sequence from each other and from BDC 12-4.1 (Fig. S5). Based on mutational and truncational analyses of the insulin peptide, AS91 and AS150 were thought to recognize the insulin peptide bound to IA^{g7} in register 1 or 2, respectively, whereas the specificity of I.29 had not been previous analyzed. Moreover, unlike BDC 12-4.1, studies with AS91 and AS150 suggested that they required peptides that extended N terminally to B:10 (15). Therefore, we generated IA^{g7} complexes with the extended B:10–23 peptide trapped in register 1, 2, or 3. Once again, the optimized anchors of Arg at p1 and Glu at p9 were used to trap the peptide in each register, but in this case, the natural Cys at B:19 of the peptide was present (Fig. 2 and Fig. S6). For comparison, we also generated an IA^{g7} complex linked to the unmodified B:10–23 peptide. As before, all of the recombinant complexes expressed well on the surface of insect cells (Fig. S4*B*).

ICAM/$B7^+$ insect cells expressing the complexes and various controls were assessed for their ability to stimulate the four T-cell hybridomas (Fig. 2). All four hybridomas responded maximally to immobilized anti-Cβ Mab (21). Thus they had approximately the same response to strong TCR cross-linking. Also, all four hybridomas responded to a soluble form of the natural insulin peptide presented by NOD spleen antigen-presenting cells (APCs). BDC 12-4.1 and AS91 responded weakly, whereas AS150 and I.29 responded strongly, suggesting differences in the affinity of these T cells for the IA^{g7} peptide complex. None of the hybridomas responded to IA^{g7} linked to an irrelevant HEL peptide. The more strongly reactive AS150 and I.29 responded to insect cells presenting IA^{g7} linked to the unmutated B:10–23 peptide, but the more weakly reactive BDC 12-4.1 and AS91 did not, presumably reflecting the heterogeneous peptide registers and the better antigen presentation function of the natural splenic APCs compared with the insect cells. Most importantly, when tested with IA^{g7} linked to each of the three register-trapped versions of the B:10–23 peptide, none of T cells responded to either register 1 or 2, but all responded to the register 3 version just as well as they did to the soluble insulin peptide presented by NOD APCs. Thus all these hybridomas recognized the insulin peptide bound to IA^{g7} in register 3, even though previous studies have suggested otherwise (15).

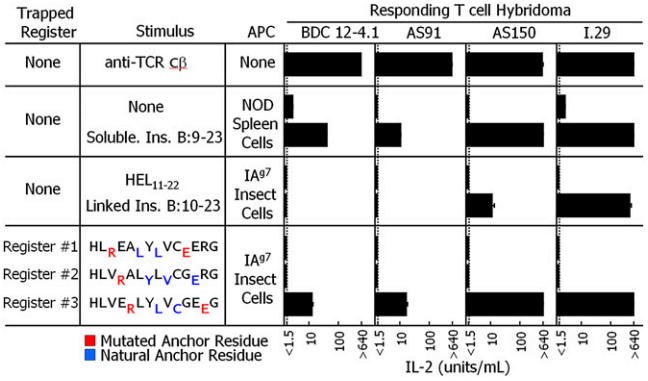

Fig. 2. Four independent insulin B-chain responsive T cells recognize the peptide bound to IA^{g7} in register 3. Triplicate culture wells of the BDC 12-4.1, AS91, AS150, and I.29 insulin B-chain responsive $CD4^+$ T-cell hybridomas were stimulated with an immobilized anti-Cβ Mab (five experiments), NOD spleen cells with or without 50 μg/mL of soluble insulin B:9–23 peptide (two experiments), ICAM/$B7^+$-infected insect cells expressing IA^{g7} linked to the control hen egg lysozyme (HEL) peptide or to the unmutated B:12–23 peptide (three experiments), or ICAM/$B7^+$-infected insect cells expressing IA^{g7} linked to each of three trapped versions (Fig. S6) of the insulin B:10–23 peptide (three experiments). The responses of the hybridomas were assessed by IL-2 production, and the average response and SEM is shown.

Trapping Dramatically Improves Insulin Peptide Binding in Register 3. Because these findings were unexpected, we tested whether our register-trapping strategy had actually improved peptide binding in register 3. We synthesized soluble minimal-core nonamer insulin peptides corresponding to registers 1, 2, and 3 with either the natural anchors at p1 and p9 or with the p1 and p9 positions optimized to Arg and Glu, respectively. To avoid peptide dimerization, we changed the B19 Cys to Ala in all of the peptides. We accessed the ability of the peptides to bind to IA^{g7} based on their relative ability to inhibit the binding of a biotinylated HEL peptide to soluble IA^{g7}. The unbiotinylated HEL peptide was used as a positive control and a peptide from moth cytochrome *c* (MCC) was used as a negative control. The results of a typical experiment are shown in Fig. 3*A*. The inhibition curves from this and two other experiments were combined to calculate the average inhibitory power of each peptide compared with the HEL peptide (Fig. 3*B*).

The HEL peptide was about 50- to 100-fold better than the MCC peptide in binding to IA^{g7}. The register 1 peptide bound IA^{g7} nearly as well as the HEL peptide, regardless of whether its p1 and p9 anchors were optimized. The register 2 peptide bound to IA^{g7}, but only about 1/10th as well as the register 1 peptide, despite its natural optimal Glu anchor at p9. Its binding was not improved by introducing the p1 Arg anchor. Perhaps this peptide binds suboptimally because, as previously suggested, its Tyr at p4 may fit poorly into the p4 pocket of IA^{g7} (22). As predicted, the register 3 peptide with its natural anchors bound IA^{g7} very poorly. Importantly, optimization of the register 3 anchors to p1Arg and p9Glu dramatically improved its binding to IA^{g7} binding. These results confirmed the conclusions of Levisetti et al. (15) that the preferred binding registers for the insulin peptide are registers 1 and 2, and also demonstrated that the register-trapping strategy converts the register 3 peptide from a very poorly to a very strongly IA^{g7}-binding peptide.

The properties of the IA^{g7} peptide- binding pockets predict that in the optimized register 3 peptide, the Arg-to-Glu mutation at p9 should be much more important than the Ala-to-Arg mutation at p1. To test this prediction we compared the IA^{g7} binding of the unmutated and doubly mutated peptides to two additional nonamer peptides, in which only one of the two mutations was introduced. The single mutation of p1 Ala to Arg did not improve binding, but the peptide with just the Arg-to-Glu mutation at p9 bound as well as the doubly mutated peptide, again confirming the rationale for fixing the register-3 binding by the p9 mutation (Fig. 3*C*).

Trapping Confirmed by Disulfide Bond Formation Between the Peptide and IA^{g7}. To exclude the possibility that the p1Arg/p9Glu version of the register 3 peptide was bound and presented by IA^{g7} in some unexpected way, we engineered cysteines both into the peptide, covalently linked to the IA^{g7} β-chain, and into the IA^{g7} α-chain such that the two cysteines should form a disulfide only were the peptide trapped in register 3. Based on the solved crystal structure of IA^{g7} bound to a GAD peptide (10), we identified two different sites for these cysteines. First, for the natural B:10–23 peptide, binding in register 3 would place its cysteine (B:19) in the p6 pocket of IA^{g7} where it could disulfide bond to a Cys substituted for IA^{g7} αAsn62 (Fig. 4*A*). Alternately, a Cys substitution at αAsn72 could form a disulfide with a Cys placed at the p11 position of the peptide/linker (Fig. 4*B*), as previously described for MHCI plus peptides (23).

To find out if the predicted disulfide bonds formed, we modified the register 3-trapped peptide to introduce these pairs of cysteines

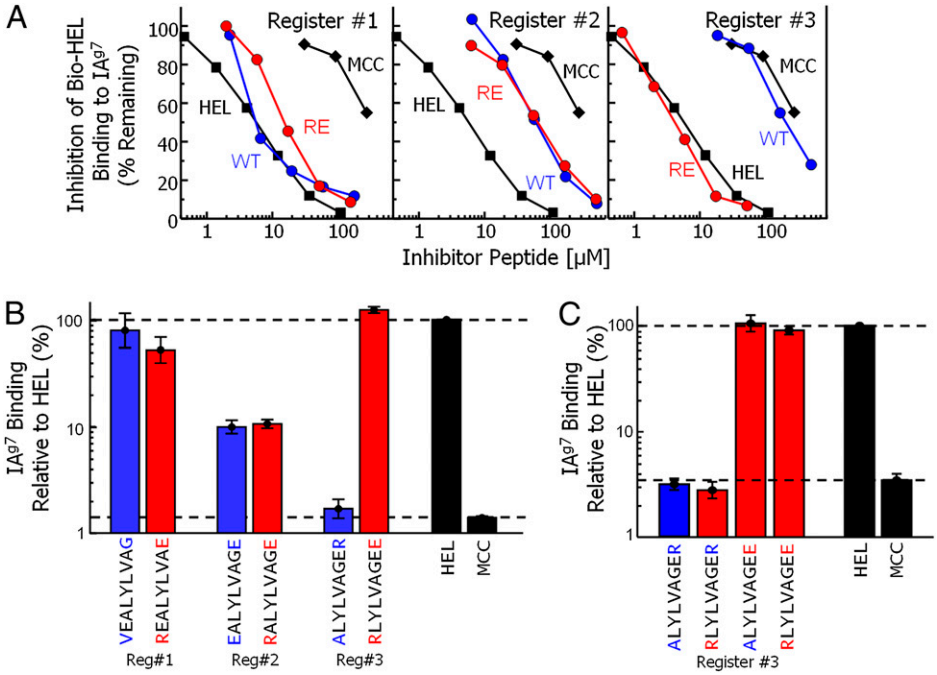

Fig. 3. The p9 Arg-to-Glu mutation dramatically improves the binding of a register 3 peptide to IA^{g7}. (*A*) Various concentrations of either unmutated (blue) or p1Arg/p9Glu (red) versions of the minimal nonamer peptides for registers 1, 2, and 3 of the B:12–23(19A) peptide were compared with a HEL peptide (positive control, black squares) and an MCC peptide (negative control, black diamonds) for the ability to inhibit the binding of a biotinylated HEL peptide to soluble IA^{g7}. The panels show the percent of biotinylated HEL peptide remaining bound to IA^{g7} vs. the dose of inhibitor. The results are for a representative experiment. (*B*) The experiment described in *A* was performed three times. In each experiment the inhibition curve for each peptide was compared with the curve obtained with the HEL peptide to determine its IA^{g7} binding ability relative to HEL expressed as a percent. The results presented are the average value for the three experiments with the SEM. Blue bars, unmutated peptides; red bars, p1Arg/p9Glu peptides; black bars, control peptides. (*C*) The relative ability of the unmutated register-3 nonamer peptide to bind to IA^{g7} (blue bar) was compared with register-3 peptides bearing p1Arg and/or p9Glu (red bars) and to the HEL and MCC control peptides (black bars), as in *A* and *B*. The results are the average ± SEM of three experiments.

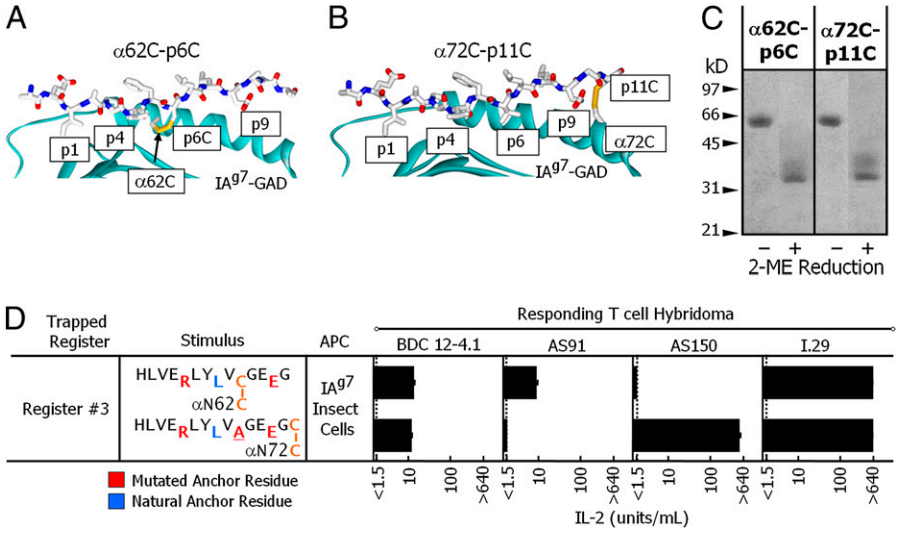

Fig. 4. Confirmation by disulfide bond formation that the insulin peptide is trapped in register 3. The structure of IA^{g7} bound to a GAD peptide (PDB ID code 1ES0) (11) was used to model (Swiss PDB Viewer) (39) cysteines replacing the amino acids either at peptide p6 and IA^{g7} α62Asn (*A*) or at peptide p11 and IA^{g7} α72Ile (*B*). In both cases, the distance and orientation of the cysteines predict the formation of a disulfide bond. (*C*) The stimulating register 3 complex in Fig. 2 was altered to remove its baculovirus gp64 transmembrane anchor. The complex was mutated to introduce a Cys into the IA^{g7} α chain at either 62Asn or 72Ile. The peptide-encoding region of the α72Ile>Cys complex was further mutated to convert the Cys at p6 to Ala and the Ala at p11 to Cys (Fig. S6). Infected insect cells were infected with baculovirus encoding for each complex and the soluble IA^{g7} purified from the culture supernatant. The soluble IA^{g7} complexes were analyzed by SDS/PAGE under nonreducing and reducing conditions. The gels were stained with Coomassie blue. (*D*) The baculovirus gp64 transmembrane anchor was restored to each complex shown in *C*, allowing expression via baculovirus on ICAM/B7$^+$ insect cells, which were used to stimulate the four T-cell hybridomas. The responses were assessed by IL-2 production, and the average of three experiments with triplicate wells are shown with the SEM.

and analyzed soluble forms of both complexes by SDS/PAGE (Fig. 4*C*). Normally, the α- and β-chains of soluble MHCII molecules readily dissociate when boiled in SDS/PAGE sample buffer. However, in these complexes, because the peptide is already covalently linked to the IA^{g7} β-chain, a disulfide bond between the α-chain and the peptide should prevent dissociation unless the complex is intentionally reduced. In the absence of reduction, virtually all of the register 3-trapped IA^{g7} complexes from both constructions migrated with an apparent mass of ∼64 kDa, the predicted MW of the disulfide-linked αβ IA^{g7} heterodimer. Upon reduction, these complexes separated into individual lower MW chains, proving the higher MW complex was due to the formation of a disulfide bond. These results confirmed that the optimized anchor residues had trapped nearly all of the peptide in register 3.

Finally, we tested the ability of the surface-bound versions of these disulfide-linked complexes to stimulate the four T-cell hybridomas. Both complexes yielded good surface expression of IA^{g7} on the insect cells (Fig. S4*C*). All four hybridomas responded to at least one of the complexes, confirming that they indeed recognized the peptide bound in register 3 (Fig. 4*D*). However, AS150 failed to respond to the p6-α62 disulfide-linked complex, and AS91 failed to respond to the p11-α72 disulfide-linked complex, despite the fact that they both responded to the nondisulfide version. These failures probably occurred because, even when bound in the appropriate register, local constraints in the exact conformation of the peptide backbone affected the fine structure of the surface-exposed portion of the peptide detected by some, but not all, T cells (24).

Discussion

A number of hypotheses have been suggested to account for the linkage between MHCII polymorphisms and autoimmunity in general and between IA^{g7} and T1D in the NOD mouse in particular. The longest-standing idea is that IA^{g7} binds and presents the relevant pancreatic antigenic peptides, including those from insulin, better than other MHCII alleles do (6). An alternate hypothesis suggests that IA^{g7} binds peptides in general less well than other IA alleles do because the structure of its p9 pocket destabilizes binding of many peptides, leading to a general decrease in presentation of self-antigens during thymic negative selection, allowing autoimmune T cells to escape into the periphery (25, 26).

Our data led us to propose a third hypothesis, that rather than having a generalized peptide-presentation defect, IA^{g7} presents just the relevant autoimmune epitopes poorly. This notion is not tenable if the target of diabetogenic T cells in NOD T1D is the B:9–23 insulin peptide in the favored registers, 1 or 2 (15). However, the results shown here, demonstrating that the target of four unrelated, diabetogenic, insulin-specific T cells, two of which were previously thought to bind B:12–23 in registers 1 and 2, is actually B:12–23 bound in the unfavored register 3, strongly support this third idea. Thus we conclude that T cells recognizing register 1 and 2 actually do not contribute to disease, presumably because they have been effectively deleted by sufficient antigen presentation in the thymus, whereas those recognizing register 3 escape because of poor thymic presentation. Because similar polymorphisms that directly affect peptide binding are also present in human T1D susceptibility MHCII alleles (1, 4, 22), our findings in the NOD mouse raise the possibility that they may play the same role in T1D patients.

The suggestion that poor presentation of particular peptides leads to the escape of autoreactive T cells from the thymus raises the question of how these T cells overcome this problem to cause disease peripherally in the pancreas. There are a number of possibilities. The simplest idea might be that the difference lies in antigen dose. Insulin is expressed in the thymus, regulated in part by the transcriptional regulator Aire (27). Apparently, this level of expression is insufficient for effective tolerance in NOD mice. However, overexpression of proinsulin in NOD mice via a transgene prevents the development of T1D, presumably due to a better level of presentation in the thymus (28). In the pancreas, insulin expression is extremely high. This increased dose alone might push register-3 insulin presentation to the threshold required to activate T cells that have escaped thymic deletion, thus initiating T1D.

Second, some difference in peripheral processing and/or interaction with IA^{g7} might improve presentation of insulin in register 3 in the pancreas. Such differences could be caused by destruction of registers 1 and/or 2, but not register 3, by differential processing in peripheral tissues, leaving register 3 to bind IA^{g7} uncompeted. Finally, Unanue and coworkers (29, 30) have reported that even with a given peptide-binding register, peptide conformation is not homogeneous. They describe two peptide/MHCII conformations, A and B, dependent on the pathway of peptide loading, which can be discriminated by individual T cells (29). Their recent paper (30) suggests that pathogenic T cells in NOD T1D recognize the B form of insulin bound to IA^{g7} and that this form is preferentially generated in the pancreas. Therefore a difference between the ratio of these two forms between thymus and pancreas could explain the peripheral activation of thymic escapees.

There are other examples of self-peptides involved in autoimmunity that bind to MHCII in unusual ways and/or are recognized by $CD4^+$ T cells in an unconventional way. For example, WE14, a 14-aa peptide that results from the natural processing of the β-cell granule protein chromogranin A (31), is bound to IA^{g7} such that only its first five amino acids lie in the binding groove, filling positions p5–p9. The other nine amino acids extend from the binding groove and contribute to IA^{g7} binding in some essential, but unknown, fashion, providing an example of an autoantigen that might require tissue-specific processing to generate the relevant epitope. Another example is the myelin basic protein peptide recognized in mouse experimental autoimmune encephalomyelitis in IA^u mice (16, 32). Like the WE14 peptide, when recognized by $CD4^+$ T cells, this peptide only partially fills the antigen-binding groove of IA^u. Finally, Li et al. (33) have shown the very unusual engagement of a complex of HLA-DR51 and a myelin basic protein peptide by a human TCR. The TCR footprint is extremely tilted toward the N-terminal end of the peptide, interacting with amino acids outside of the binding groove at p−1, p−2, and p−4, and lacking the usual engagement with the MHCII α-helices and center of the peptide. Together, these findings suggest that T-cell thymic tolerance to self-antigens may be in general very efficient, and that only rare antigens that are presented or recognized in unconventional ways allow the development of autoimmunity.

It is not immediately apparent why previous mutational and truncation data indicated register 1 or register 2, rather than register 3, to be the recognized binding registers for the insulin peptide in NOD T1D (15). It is possible that competition among the binding registers obscured the interpretation of the results of the previous experiments. The most surprising data in this previous paper was that some T cells, including AS91 and AS150, responded to some versions of the peptide that lacked the p9Arg of register 3, leaving peptides that would not completely fill the binding groove. However, as discussed previously, there is precedent for autoimmune T-cell recognition of foreshortened self-peptides. Moreover, perhaps more is gained, in terms of register-3 recognition, by eliminating the unfavored p9Arg than is lost by the absence of the p9 anchor altogether.

Finally, our findings illustrate the difficulty in determining the relevant mode of MHCII binding of self-peptides involved in autoimmunity, especially when peptides can shift and bind in multiple overlapping registers. Traditional truncation/mutation approaches may not be sufficient to identify the actual epitopes, because inferior binding registers may have to compete with irrelevant overlapping favorable binding registers (16, 34). In these cases, additional approaches, such as the register-trapping and disulfide formation approaches described herein may be needed to supply more direct evidence for the relevant binding registers recognized by self-reactive T cells. This approach may also be useful in defining the functional register of conventional foreign antigen peptides that are known to bind to an MHCII molecule in multiple registers.

Materials and Methods

T-Cell Hybridomas. The BDC 12-4.1 T-cell hybridoma was created by fusing BW5147 α/β T cells with BDC 12-4.1 $RAG^{-/-}$ splenocytes (18). The AS91 and AS150 T-cell hybridomas (15), as well as the I.29 T-cell hybridoma, were generous gifts from Matteo Levisetti (University of Washington, St. Louis). T-cell hybridomas were grown in modified SME media (35) (Invitrogen).

IA^{g7}-Linked Peptide Complexes. The IA^{g7} α- and β-chains were placed under the p10 and pH promoters in the pBacp10pH baculovirus transfer vector, respectively (19, 20, 36). The α-chain was terminated following residue α182E to remove the transmembrane domain, and attached to a basic leucine zipper (37). The β-chain contained a peptide with a C-terminal flexible linker (GGGSLVPRGSGGGGS) inserted between the signal peptide and the N terminus of the β1 domain. The β2 domain was truncated at residue β190Q and attached to an acid leucine zipper (37) followed by the baculovirus gp64 transmembrane domain. Soluble versions of the complexes were achieved by removal of the gp64 transmembrane domain on the β-chain and the addition of the TCRCα epitope tag (DATLTEKSFETDMNLNFQNLSVN) to the C terminus of the α-chain.

Generation of Recombinant Baculovirus. IA^{g7}-containing baculoviruses were generated by homologous recombination between the transfer vector and linearized Safire baculovirus DNA (Oribigen) using the manufacturer's calcium phosphate cotransfection protocol and SF9 insect cells. A virus stock was collected after 10 d.

Expression and Purification of IA^{g7} Complexes. Soluble IA^{g7}-linked peptide complexes were produced in spinner flasks by infecting 5.2×10^8 Hi-5 cells (MOI ~3) in 250 mL plain Grace's medium. After 2 h, the culture was supplemented with 550 mL of TMN-FH media, incubated overnight at 27 °C, and then moved to 19 °C for 6 d. Supernatant was harvested and cleared of debris by centrifugation. Soluble IA^{g7} was immunoaffinity purified using Mab, AD0124.5 (anti-TCRCα epitope), coupled Sepharose, eluted in 50 mM carbonate buffer (pH 10.4), and adjusted to a neutral pH using 0.15 vol 1 M Tris (pH 6.9). The protein was buffer exchanged into PBS with 0.1% azide by centrifugation, Amicon Ultra 30 kDa. The resulting protein isolate was subject to FPLC size exclusion Superdex 200 chromatography (GE Healthcare) to remove aggregate or contaminating proteins.

SDS/PAGE Electrophoresis. SDS/PAGE analysis was carried out using a 12.5% Phastgel (GE Healthcare). An aliquot containing 1 μg/μL of protein was boiled in an equal volume of 2× SDS/PAGE sample buffer with and without the addition of 2-mercaptoethanol. Approximately 0.5 μg of total protein was loaded in each lane.

T-Cell Stimulation Assays. Viruses expressing IA^{g7} with a transmembrane domain were used to infect ICAM/$B7^+$-expressing SF9 cells (20). Three days after infection the cells were used as artificial APCs. In 250 μL of complete tumor media, 1×10^5 T-cell hybridomas were cocultured with 3×10^4 infected Sf9 cells (35). After 24 h, the supernatants assayed for IL-2 using IL-2–dependent HT-2 cell line (38).

Binding of Peptides to IA^{g7}. The binding of peptides to soluble IA^{g7} was determined in a peptide competition binding assay as previously described (31). Briefly, soluble IA^{g7} with a covalent hen egg lysozyme peptide (aa11-22, HEL) (Fig. S6) was prepared. The purified protein was treated with thrombin to cleave at a thrombin site in the linker connecting the peptide to the IA^{g7} β-chain (36). Samples (0.5 μg) were incubated with a limiting amount of a soluble biotinylated version of $pHEL_{11-22}$, biotin-GGGMKRHGLDNYRGYSL (11 μM), either alone or in the presence of various concentrations of potential competitors peptides in 15 μL of pH 5.3 buffer overnight at room temperature. An unbiotinylated HEL peptide was used as the positive control, and a moth cytochrome *c* peptide (MCC_{88-103}) peptide was used as the negative control. The sample was diluted to 100 μL PBS in a well of a 96-well ELISA plate coated with an IA^{g7} monoclonal antibody, OX6 (BD Pharmaceuticals). The captured IA^{g7} was washed several times with PBS, and the bound bio-pHEL detected with akaline phosphatase-coupled Extravidin (Sigma) and *o*-nitrophenol phosphate. The binding inhibition curves were compared to calculate the binding ability of the inhibitor peptides relative to the HEL peptide.

ACKNOWLEDGMENTS. We thank Drs. M. Levisetti and E. Unanue (Washington University, St. Louis) for generously providing the AS91, AS150, and I.29 insulin-reactive T-cell hybridomas and Drs. B. K. B Stadinski, E. Clambey, and M. Macleod for critical reading and discussions. This work was supported by National Institutes of Health Grants 5 U19-AI05086, AI-17134, AI-18785 AI050864, DK55969, and DK057516 and Juvenile Diabetes Research Foundation Grant 4-2007-1056.

1. Erlich H, et al.; Type 1 Diabetes Genetics Consortium (2008) HLA DR-DQ haplotypes and genotypes and type 1 diabetes risk: Analysis of the type 1 diabetes genetics consortium families. *Diabetes* 57:1084–1092.
2. Prochazka M, Leiter EH, Serreze DV, Coleman DL (1987) Three recessive loci required for insulin-dependent diabetes in nonobese diabetic mice. *Science* 237:286–289.
3. Todd JA, Bell JI, McDevitt HO (1987) HLA-DQ beta gene contributes to susceptibility and resistance to insulin-dependent diabetes mellitus. *Nature* 329:599–604.
4. Suri A, Walters JJ, Gross ML, Unanue ER (2005) Natural peptides selected by diabetogenic DQ8 and murine I-A(g7) molecules show common sequence specificity. *J Clin Invest* 115: 2268–2276.
5. Reich EP, et al. (1994) Self peptides isolated from MHC glycoproteins of non-obese diabetic mice. *J Immunol* 152:2279–2288.
6. Suri A, et al. (2002) In APCs, the autologous peptides selected by the diabetogenic I-Ag7 molecule are unique and determined by the amino acid changes in the P9 pocket. *J Immunol* 168:1235–1243.
7. McFarland BJ, Beeson C (2002) Binding interactions between peptides and proteins of the class II major histocompatibility complex. *Med Res Rev* 22:168–203.
8. Hattori M, et al. (1986) The NOD mouse: Recessive diabetogenic gene in the major histocompatibility complex. *Science* 231:733–735.
9. Acha-Orbea H, McDevitt HO (1987) The first external domain of the nonobese diabetic mouse class II I-A beta chain is unique. *Proc Natl Acad Sci USA* 84:2435–2439.
10. Latek RR, et al. (2000) Structural basis of peptide binding and presentation by the type I diabetes-associated MHC class II molecule of NOD mice. *Immunity* 12:699–710.
11. Corper AL, et al. (2000) A structural framework for deciphering the link between I-Ag7 and autoimmune diabetes. *Science* 288:505–511.
12. Daniel D, Gill RG, Schloot N, Wegmann D (1995) Epitope specificity, cytokine production profile and diabetogenic activity of insulin-specific T cell clones isolated from NOD mice. *Eur J Immunol* 25:1056–1062.
13. Abiru N, et al. (2000) Dual overlapping peptides recognized by insulin peptide B:9-23 T cell receptor AV13S3 T cell clones of the NOD mouse. *J Autoimmun* 14:231–237.
14. Burton AR, et al. (2008) On the pathogenicity of autoantigen-specific T-cell receptors. *Diabetes* 57:1321–1330.
15. Levisetti MG, Suri A, Petzold SJ, Unanue ER (2007) The insulin-specific T cells of nonobese diabetic mice recognize a weak MHC-binding segment in more than one form. *J Immunol* 178:6051–6057.
16. Bankovich AJ, Girvin AT, Moesta AK, Garcia KC (2004) Peptide register shifting within the MHC groove: Theory becomes reality. *Mol Immunol* 40:1033–1039.
17. Anderton SM (2004) Post-translational modifications of self antigens: Implications for autoimmunity. *Curr Opin Immunol* 16:753–758.
18. Zhang L, Nakayama M, Eisenbarth GS (2008) Insulin as an autoantigen in NOD/human diabetes. *Curr Opin Immunol* 20:111–118.
19. Crawford F, et al. (2006) Use of baculovirus MHC/peptide display libraries to characterize T-cell receptor ligands. *Immunol Rev* 210:156–170.
20. Crawford F, Huseby E, White J, Marrack P, Kappler JW (2004) Mimotopes for alloreactive and conventional T cells in a peptide-MHC display library. *PLoS Biol* 2: 523–533.
21. Kubo RT, Born W, Kappler JW, Marrack P, Pigeon M (1989) Characterization of a monoclonal antibody which detects all murine alpha beta T cell receptors. *J Immunol* 142:2736–2742.
22. Lee KH, Wucherpfennig KW, Wiley DC (2001) Structure of a human insulin peptide-HLA-DQ8 complex and susceptibility to type 1 diabetes. *Nat Immunol* 2:501–507.
23. Truscott SM, et al. (2007) Disulfide bond engineering to trap peptides in the MHC class I binding groove. *J Immunol* 178:6280–6289.
24. Kersh GJ, et al. (2001) Structural and functional consequences of altering a peptide MHC anchor residue. *J Immunol* 166:3345–3354.
25. Carrasco-Marin E, Shimizu J, Kanagawa O, Unanue ER (1996) The class II MHC I-Ag7 molecules from non-obese diabetic mice are poor peptide binders. *J Immunol* 156: 450–458.
26. Stratmann T, et al. (2000) The I-Ag7 MHC class II molecule linked to murine diabetes is a promiscuous peptide binder. *J Immunol* 165:3214–3225.
27. Mathis D, Benoist C (2009) Aire. *Annu Rev Immunol* 27:287–312.
28. French MB, et al. (1997) Transgenic expression of mouse proinsulin II prevents diabetes in nonobese diabetic mice. *Diabetes* 46:34–39.
29. Pu Z, Lovitch SB, Bikoff EK, Unanue ER (2004) T cells distinguish MHC-peptide complexes formed in separate vesicles and edited by H2-DM. *Immunity* 20:467–476.
30. Mohan JF, et al. (2010) Unique autoreactive T cells recognize insulin peptides generated within the islets of Langerhans in autoimmune diabetes. *Nat Immunol* 11: 350–354.
31. Stadinski BD, et al. (2010) Chromogranin A is an autoantigen in type 1 diabetes. *Nat Immunol* 11:225–231.
32. He XL, et al. (2002) Structural snapshot of aberrant antigen presentation linked to autoimmunity: The immunodominant epitope of MBP complexed with I-Au. *Immunity* 17:83–94.
33. Li Y, et al. (2005) Structure of a human autoimmune TCR bound to a myelin basic protein self-peptide and a multiple sclerosis-associated MHC class II molecule. *EMBO J* 24:2968–2979.
34. Landais E, et al. (2009) New design of MHC class II tetramers to accommodate fundamental principles of antigen presentation. *J Immunol* 183:7949–7957.
35. Kappler JW, Skidmore B, White J, Marrack P (1981) Antigen-inducible, H-2-restricted, interleukin-2-producing T cell hybridomas. Lack of independent antigen and H-2 recognition. *J Exp Med* 153:1198–1214.
36. Kozono H, White J, Clements J, Marrack P, Kappler J (1994) Production of soluble MHC class II proteins with covalently bound single peptides. *Nature* 369:151–154.
37. O'Shea EK, Lumb KJ, Kim PS (1993) Peptide 'Velcro': Design of a heterodimeric coiled coil. *Curr Biol* 3:658–667.
38. Walker E, Warner NL, Chesnut R, Kappler J, Marrack P (1982) Antigen-specific. I region-restricted interactions in vitro between tumor cell lines and T cell hybridomas. *J Immunol* 128:2164–2169.
39. Guex N, Peitsch MC (1997) SWISS-MODEL and the Swiss-PdbViewer: An environment for comparative protein modeling. *Electrophoresis* 18:2714–2723.